Short Communication

Rice straw-based activated carbons doped with SiC for enhanced hydrogen adsorption

S. Schaefer [a], G. Muñiz [a,b,c], M.T. Izquierdo [d], S. Mathieu [a], M.L. Ballinas-Casarrubias [b], G. González-Sánchez [c], A. Celzard [a], V. Fierro [a,*]

[a] Institut Jean Lamour, UMR CNRS - Université de Lorraine n°7198, ENSTIB, 27 Rue Philippe Séguin, CS 60036, 88026 Épinal cedex, France
[b] Department of Renewable Energies and Environmental Protection, Centro de Investigacion en Materiales Avanzados (CIMAV S.C.), Chihuahua, Chih, Mexico
[c] Graduate Department, Facultad de Ciencias Quimicas, Universidad Autonoma de Chihuahua (UACH), Chihuahua, Chih, Mexico
[d] Instituto de Carboquímica (ICB-CSIC), Miguel Luesma Castán, 4, Zaragoza, E-50018, Spain

ARTICLE INFO

ABSTRACT

Activated carbons (ACs) based on rice straw (RS) were synthesised using potassium carbonate as activating agent at three different K_2CO_3/RS weight ratios. Morphological, chemical, structural as well as textural characterisations were carried out in order to establish relationships between the physicochemical properties of the materials and their hydrogen adsorption capacities. The ACs contained potassium and silicon as the main impurities. Si was identified by XRD in both phases of silicon dioxide and silicon carbide. The presence of SiC was particularly surprising due to the rather low activation temperature, much lower than what is usually required for SiC synthesis. ACs exhibited well-developed surface areas (approximatively $2000-2100$ m^2 g^{-1}) and high micropore volumes, making them suitable for hydrogen storage applications. RS-based ACs showed higher hydrogen storage capacities than those previously obtained with KOH-activated sucrose. The latter exhibited hydrogen uptakes (excess, 10 MPa, 298 K) up to 0.55 wt. %, whereas 0.65 wt. % was measured for RS-based ACs in the same conditions. The higher hydrogen capacities and isosteric heats of adsorption found here were attributed to the presence of SiC.

Introduction

The design of high-efficiency hydrogen storage systems is a bottleneck step in the development of hydrogen as an energy vector. Solid-state hydrogen storage systems, either by absorption or adsorption, have been investigated for many years. Activated carbons (ACs) are cheap, compared to more sophisticated materials such as Metal Organic Frameworks,

and are often biosourced materials exhibiting high hydrogen storage capacities at cryogenic temperatures (around 6.8 wt. % in excess at 77 K) [1]. Hydrogen excess uptake in ACs is most of the time lower than 1 wt. % near room temperature and 10 MPa [1–4]. Several strategies were applied to increase hydrogen – ACs surface interactions. Metal nanoparticle doping is the most widespread approach for inducing hydrogen chemisorption, spill-over or polarised physisorption [5–10]. The second approach consists in introducing hetero-atoms for increasing the hydrogen adsorption potential at the surface of the carbon-based materials. Thus, N and B were introduced, forming carbon nitrides, carbon boro-nitrides or even carbides, and their positive effect on hydrogen adsorption was demonstrated [11–15]. The favourable effect of silicon carbide (SiC) on hydrogen adsorption was theoretically [16] and experimentally [17,18] investigated. However, the synthesis of SiC remains uneasy due to the high temperatures required, typically in the range 1600–1900 K [19]. In addition, the interactions between hydrogen and SiC were investigated in carbon-SiC nanotubes [17,18] having low surface areas (i.e., below 100 $m^2 g^{-1}$, according to the BET method based on N_2 adsorption at 77 K). Despite the fact that these studies evidenced the possibility of using SiC-doped materials for hydrogen storage, the low surface areas of those materials limited the hydrogen uptake. Hence, SiC-containing materials of much higher specific areas might be interesting materials for hydrogen storage.

The synthesis of SiC and SiC-containing materials based on rice by-products such as rice husk and rice straw at high temperatures is well known [19–23]. Hydrogen storage in rice-based ACs has been studied at 77 K, a temperature at which pore texture is much more important than electrostatic interactions [24,25]. As far as we know, hydrogen adsorption heats of ACs containing SiC were never determined at near room temperature.

Therefore, the purpose of the present study was to elucidate whether the presence of Si in high surface area-ACs improves hydrogen adsorption near room temperature. ACs were thus prepared by K_2CO_3 activation of rice straw (RS). The corresponding hydrogen adsorption data were compared with previous results taking into account the surface area and the average pore size of the ACs. We definitely showed that SiC doping has a positive effect on hydrogen adsorption, increasing both excess uptake and heat of adsorption.

Experimental

Materials synthesis

20 g of rice straw (RS) were cut, manually ground and then impregnated for 24 h using 300 mL of a solution of potassium carbonate of the appropriate concentration in order to get the desired activation ratio. Then the mixture was left to dry at 393 K K_2CO_3 is a better activating agent than Na_2CO_3 [26,27] and it is also cheaper than KOH. In order to promote the activation effect, the activation temperature was 1173 K, higher activation temperatures being expected to promote the conversion of SiO_2 into SiC. The activation ratio (R) was defined as the K_2CO_3 to RS mass ratio, and the corresponding

samples were labelled KC-RS_R, where R was fixed to 3, 4 or 5. After impregnation, RS was put in an oven at 393 K overnight in order to evaporate water. The impregnated, dry, RS was placed in a nickel crucible and then put in a horizontal stainless steel tubular oven flushed by pure nitrogen flowing at 100 mL min^{-1}, and heated at 3 K min^{-1} up to the final temperature of 1173 K. The latter was held for 2 h, and then the sample was cooled under N_2 flow. The crucible containing the activated material was then removed from the furnace and let to oxidise slowly in air for several hours to avoid violent K oxidation upon washing. Then, the material was washed with hydrochloric acid (1 mol L^{-1}), bi-distilled water, and finally in a Soxhlet extractor for 2 days with bi-distilled water again to eliminate the remaining carbonates.

Characterisation

The textural characterisation of ACs was performed by nitrogen and carbon dioxide adsorption at 77 and 273 K, respectively, using an automatic adsorption apparatus (ASAP 2020, Micromeritics). The samples were degassed under vacuum at 423 K until the pressure stabilised around 0.2–0.4 mPa for more than 48 h. Further degassing was carried out at the measuring port for at least 6 h. Cool and warm volumes were determined after nitrogen or carbon dioxide adsorption to avoid helium entrapment in the narrowest pores. Adsorption data were treated using the Microactive software from Micromeritics. The pore size distributions (PSDs) were obtained using non-local density functional theory (NLDFT) with the Solution of Adsorption Integral Equation Using Splines (SAIEUS®) routine. SAIEUS® has the advantage of combining both CO_2 and N_2 adsorption data to get more accurate PSDs [28]. The aforementioned NLDFT method was also used to determine the surface areas, S_{NLDFT} ($m^2 g^{-1}$), by integrating the PSDs over the whole range of pore sizes [29].

Scanning Electron Microscopy (SEM) observations with secondary electrons (SE) and backscattered electrons (BSE), associated with chemical analysis using Energy-dispersive X-ray spectroscopy (EDX), were carried out. All microscopy studies were made with a FEI QUANTA600FEG equipped with a Brucker Quantax spectrometer. X-ray diffraction (XRD) patterns were collected with a Bruker D8 Advance X-ray powder diffractometer equipped with a Cu anticathode working at 40 kV and 40 mA and a scintillation detector. The diffraction patterns were obtained over a 2θ range from 10° to 80° with a step of 0.02°. The assignation of crystalline phases was performed based on Joint Committee on Powder Diffraction Standards (JCPDS) files. Ash contents were obtained after calcination in air, using a muffle oven heated at 5 K min^{-1} until the final temperature of 1073 K, which was held for 45 min.

Hydrogen adsorption experiments were carried out at 298 K using a high-pressure automatic adsorption apparatus (HPVA II, Micromeritics). The temperature was set to 293 K to measure the cold volume, and then it was changed to 298 K to measure the warm volume and to carry out hydrogen adsorption. The pressure range was 0.15–10 MPa for adsorption and 10–2 MPa for desorption. The contribution of the empty cell was systematically measured and subtracted to all data in order to improve the accuracy. The quantity of

material within the sample cell was around 0.5 g. Isosteric heats of adsorption (Qst) were calculated using three hydrogen isotherms at three different temperatures (283, 298 and 313 K). The isosteric heats Qst were calculated using the Clapeyron—Clausius equation.

Results and discussion

Chemical and textural characterisation

The ash content of RS was 19.3 wt. % on dry basis. RS ashes were mainly composed of SiO_2, but other elements like potassium or calcium could also be found [30,31]. After RS activation, ash contents were equal to 3.12, 1.42 and 1.43 wt. % for KC-RS_3, KC-RS_4, KC-RS_5, respectively. Ash content decreased when R increased due to the improved reaction of the alkali carbonate with silica during activation, followed by leaching out the products. In order to obtain some information about ash composition, the chemical mapping of KC-RS_3 was carried out by EDX. The composition obviously varied depending on the area under study, but was within the ranges: 96.0—90.1 wt. % (C), 0—4.4 wt. % (N), 3.8—6.1 wt. % (O), 0—0.4 wt. % (S), 0—2.1 wt. % (Si), 0—0.5 wt. % (K), and 0—0.4 wt. % (Na). The presence of S and N is not surprising in biosourced materials. Fig. 1 presents the results of SEM-BSE imaging, EDX mapping for Si and K, and the XRD pattern for the same material (KC-RS_3).

Fig. 1(a) shows that part of the initial SiO_2 was converted into SiC. Despite having well-defined peaks, the low intensity of the latter did not allow calculating the corresponding SiC content. SiC industrial production, especially by Acheson process, requires extremely high temperatures (i.e., >2673 K) [32]. However, SiC synthesis can also be achieved by direct carbothermal reduction in the 1573—1873 K temperature range [19], which is still much higher than the activation temperature used in the present study, 1173 K. Rice, and more generally plant-based precursors, contain metallic impurities such as Fe, Ca, K, Mg, Al and Mn, which are known to be catalysts of SiC formation [30,33]. Mg is the most efficient one for this purpose, as it allows decreasing the temperature of conversion of SiO_2 into SiC down to 873 K [34]. In the present work, RS was used as received, i.e., without acidic pre-treatment or washing. As a consequence, the metallic elements naturally present might catalyse SiC formation. Moreover, as the activation agent is K_2CO_3, its reaction with silica occurs, leading to the formation of K_2SiO_3. The latter might also catalyse SiC formation, as the same has already been demonstrated for sodium silicate (Na_2SiO_3), which reduced the SiC temperature formation by 300 K [35]. Furthermore, K_2CO_3-impregnated RS was placed inside of a nickel crucible for activation and Ni, similarly to Fe and Co, is known to catalyse SiC formation [33,36,37]. Therefore, SiC was probably produced through catalytic reactions due to the initial RS mineral content, to K_2SiO_3 formed during the process, and to nickel used as container.

The material presented a porous structure maintaining the original morphology of the initial vegetal cells (Fig. 1(b) and (c)). EDX mapping of the image of Fig. 1(d), evidencing minerals as bright zones when observed with the BSE detector, showed that K was homogeneously distributed on the surface (Fig. 1(e)), probably due to RS impregnation with K_2CO_3 before activation. Si was also present overall on the surface, but some zones were richer (Fig. 1(f)).
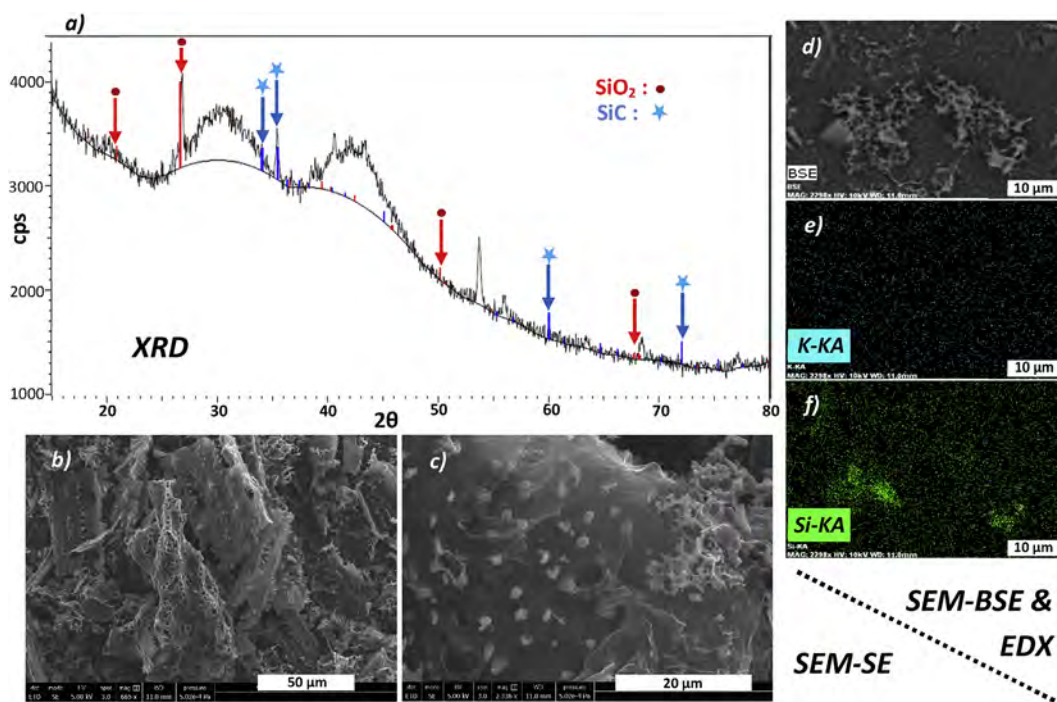

Fig. 1 — (a) XRD pattern and assignation of the SiO_2 and SiC peaks for KC-RS_3 sample, (b) and (c) SEM-SE pictures of KC-RS_3, (d) SEM-BSE picture of KC-RS_3, (e) and (f) EDX mapping of (d) for K and Si, respectively.
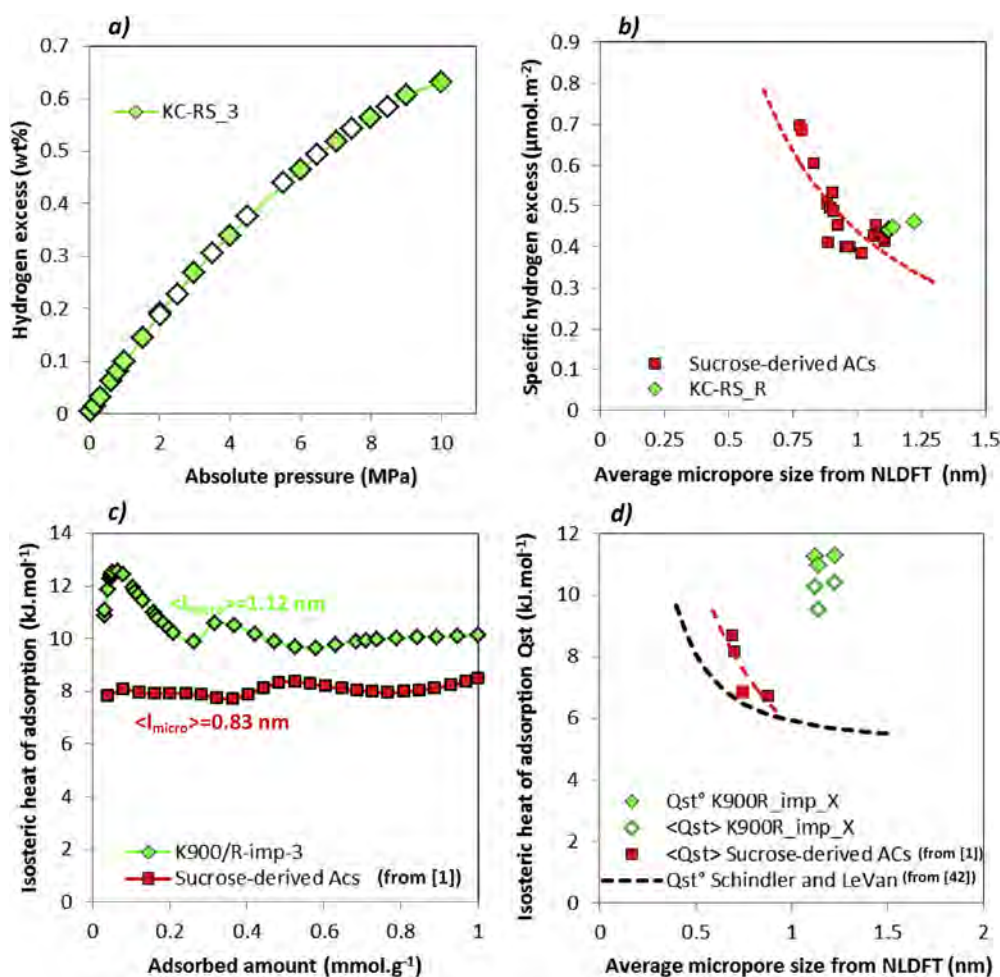
Fig. 2 − Adsorption properties of the activated carbons: (a) hydrogen adsorption-desorption isotherms on KC-RS_3 sample at 298 K (adsorption: open symbols; desorption: closed symbols); (b) comparison between the specific excess hydrogen uptake at 2 MPa and 298 K of materials synthesised here and those from a previous study [1]; (c) isosteric heats of adsorption versus excess adsorbed hydrogen amount; and (d) dependence of the average Qst (<Qst>) or near zero coverage Qst (Qst°) on the average micropore size from NLDFT [1,42].

Textural characterisation and hydrogen adsorption

PSDs obtained by NLDFT application to the N_2 and CO_2 adsorption data (not shown) allowed calculating ACs surface areas (S_{NLDFT}), which were equal to 2197, 2162 and 2034 $m^2\,g^{-1}$ for KC-RS_3, KC-RS_4 and KC-RS_5, respectively. Thus, S_{NLDFT} decreased when the activation ratio R increased due to an effect of over-activation, leading to pore widening and even pore destruction, which were observed on the corresponding PSDs. Indeed, whereas the volume of the ultramicropores (<0.7 nm) remained almost constant and equal to 0.2 $cm^3\,g^{-1}$, the volume of supermicropores (0.7−2 nm) and mesopores (>2 nm) decreased from 0.75 to 0.58 $cm^3\,g^{-1}$ and from 0.56 to 0.28 $cm^3\,g^{-1}$, respectively, when R increased from 3 to 5. The average micropore diameter was very similar for the three ACs and equal to 1.12, 1.22 and 1.13 nm for the KC-RS_3, KC-RS_4 and KC-RS_5 samples, respectively. This textural analysis allowed to evidence the mainly microporous character of the present materials.

Fig. 2(a) shows the hydrogen adsorption isotherm at 298 K of the sample KC-RS_3, taken as example. All hydrogen isotherms were completely reversible and had the typical shape reported for ACs in general [1,10]. The excess adsorbed uptakes at 10 MPa were equal to 0.63, 0.64 and 0.59 wt. % for KC-RS_3, KC-RS_4, and KC-RS_5 samples, respectively. No hysteresis was found, suggesting that neither chemisorption nor absorption took place in the materials. As a consequence, the adsorption was due to physisorption only. Dividing adsorbed amount values by the specific surface area gave specific excess values ($\mu mol\,m^{-2}$), which were represented as a function of average micropore sizes. This a common technique to compare hydrogen storage performances, which was previously reported in the literature [38].

Thus, Fig. 2(b) compares the specific excess values of hydrogen uptake measured on the materials synthesised here with those of ACs based on sucrose activated with KOH [1]. RS-based ACs exhibited slightly higher values than those based on sucrose. This might be due to the increase of the adsorption potential due to the presence of SiC [16], similarly to what had been shown with some metallic heteroatoms. Thus, K, Na or Li are well-known to enhance hydrogen adsorption when those metals are located at the surface of a carbon adsorbent,

inducing local charges due to the significant differences of electronegativity between the carbon support and the metal. This phenomenon has been theoretically and experimentally described for K and Li, and is known under the names of strong physisorption or polarised physisorption [8,9,39—41].

The nature of the carbide bond might also explain an enhanced hydrogen adsorption. Carbide bonds indeed have a heteropolar nature that implies local charges on the carbide, and which can induce a dipole on hydrogen molecules approaching the adsorbent surface and may lead to enhanced adsorption [16,43]. Although chemisorption could occur on SiC, mostly at high temperature [44—46] as on alkali-containing carbon materials [17,47], neither steps at low pressure nor hysteresis were found on the adsorption isotherms. Thus, the enhancement of hydrogen adsorption should be due to strong or polarised physisorption only. In order to investigate this assumption, isosteric heats Q_{st} were determined based on the hydrogen adsorption—desorption isotherms carried out for each AC at 283, 298 and 313 K.

Fig. 2(c) shows the dependence of the isosteric heats Q_{st} with the adsorbed amount for the KC-RS_3 material and a sucrose-derived AC, having average micropore diameters of 1.12 nm and 0.7 nm, respectively. The isosteric heats of adsorption Q_{st} of sucrose activated with KOH was given for the sake of comparison. For the RS-derived AC, Q_{st} decreased as the adsorbed amount increased due to the fact that the adsorption potential normally decreases as the coverage increases. This behaviour is typical of hydrogen adsorption on porous carbons. The usual values of isosteric heats Q_{st} for graphene are within the range 2—6 kJ mol^{-1} [48,49]. The values obtained here are thus far above this range, showing again that a classical physisorption is not the only phenomenon that occurred. The isosteric heat Q_{st} of sucrose-derived AC, activated with KOH using a W = 3 ratio, was lower than that of KC-RS_3 in the whole coverage range, despite the fact that the average pore diameter was narrower for the sucrose-derived AC. Therefore, the polarising effect was not only due to K, and Si should also have an effect.

Schindler and LeVan modelled hydrogen adsorption in graphitic carbon with slit-shaped pores, and showed an inverse dependence between isosteric heats of adsorption Q_{st} and pore sizes [42]. Fig. 2(d) shows the comparison between the values predicted by the model of Schindler and LeVan with those determined on KOH-activated sucrose on the one hand, and those determined in this study (KC-RS_R) on the other hand. The values of Q_{st} are shown as average (<Q_{st}>) or as low-coverage isosteric heats of adsorption Q_{st} ($Q_{st}°$). $Q_{st}°$ values were around 11—12 kJ mol^{-1} and should correspond to the interaction of hydrogen with the most energetic sites of the ACs. <Q_{st}> were still significantly high, around 10 kJ mol^{-1}, compared to the values obtained for the activated carbon derived from sucrose (i.e., between 7 and 9 kJ mol^{-1}) and to the theoretical values from Schindler and LeVan [42], around 6—7 kJ mol^{-1}. Due to these higher heats of adsorption Q_{st}, hydrogen storage was significantly enhanced in the present ACs, from 0.55 to 0.65 wt. % (excess, 10 MPa, 298 K), compared to ACs of similar average pore diameter. Such hydrogen storage capacities might probably be improved further if the average pore diameter was narrower. A possible strategy could therefore be the activation of rice by-products with KOH that might produce higher surface areas as well as a PSD shifted to narrower pores [50—52].

Conclusion

Rice straw (RS) was activated with potassium carbonate to produce ACs having surface areas as high as 2197 m^2 g^{-1}. These ACs had a significant ash content (1.42—3.12 wt. %), mainly due to the silica content of the precursor. Si and K contents at the AC surface were determined by SEM-EDX. Si was up to 4 times more abundant (2.1 wt. %) on the surface than K (0.5 wt. %), and was present as both SiO_2 and SiC phases. As far as we know, this is the first time that SiC is observed after chemical activation at relatively low temperature (1173 K). The presence of SiC can be explained by different catalytic reactions, and especially through the formation of K_2SiO_3. Hydrogen adsorption on RS-derived ACs was totally reversible and therefore entirely attributable to physisorption. Due to the presence of SiC and K, polarised adsorption of hydrogen was expected and was confirmed by the high values of isosteric heat of adsorption Q_{st} near room temperature, in the range 9—12 kJ mol^{-1}. This produced a significantly increase of excess hydrogen uptake, from 0.55 to 0.65 wt. % at 10 MPa and 298 K, compared to non-doped ACs having similar average pore diameters.

REFERENCES

[1] Fierro V, Szczurek A, Zlotea C, Mareche JF, Izquierdo MT, Albiniak A, et al. Experimental evidence of an upper limit for hydrogen storage at 77 K on activated carbons. Carbon 2010;48(7):1902—11.

[2] Schaefer S, Fierro V, Izquierdo MT, Celzard A. Assessment of hydrogen storage in activated carbons produced from hydrothermally treated organic materials. Int J Hydrogen Energy 2016;41(28):12146—56.

[3] Sircar S, Wang C-Y, Lueking AD. Design of high pressure differential volumetric adsorption measurements with increased accuracy. Adsorp J Int Adsorpt Soc 2013;19(6):1211—34.

[4] Xia K, Hu J, Jiang J. Enhanced room-temperature hydrogen storage in super-activated carbons: the role of porosity development by activation. Appl Surf Sci 2014;315:261—7.

[5] Stuckert NR, Wang L, Yang RT. Characteristics of hydrogen storage by spillover on Pt-Doped carbon and catalyst-bridged metal organic framework. Langmuir 2010;26(14):11963—71.

[6] Psofogiannakis GM, Froudakis GE. Fundamental studies and perceptions on the spillover mechanism for hydrogen storage. Chem Commun 2011;47(28):7933–43.

[7] Zhao W, Fierro V, Zlotea C, Izquierdo MT, Chevalier-Cesar C, Latroche M, et al. Activated carbons doped with Pd nanoparticles for hydrogen storage. Int J Hydrogen Energy 2012;37(6):5072–80.

[8] Duclaux L, Los S, Azais P, Pellenq R, Breton Y, Isnard O. Deuterium adsorption in carbon single walled carbon nanotubes doped by lithium and potassium: adsorption isotherms and in situ neutron diffraction. J Phys Chem Solids 2006;67(5–6):1122–6.

[9] Pellenq RJM, Marinelli F, Fuhr JD, Fernandez-Alonso F, Refson K. Strong physisorption site for H-2 in K- and Li-doped porous carbons. J Chem Phys 2008;129(22):224701.

[10] Schaefer S, Fierro V, Szczurek A, Izquierdo MT, Celzard A. Physisorption, chemisorption and spill-over contributions to hydrogen storage. Int J Hydrogen Energy 2016;41(39):17442–52.

[11] Kang KY, Lee BI, Lee JS. Hydrogen adsorption on nitrogen-doped carbon xerogels. Carbon 2009;47(4):1171–80.

[12] Zhao W, Fierro V, Fernandez-Huerta N, Izquierdo MT, Celzard A. Hydrogen uptake of high surface area-activated carbons doped with nitrogen. Int J Hydrogen Energy 2013;38(25):10453–60.

[13] Xia Y, Walker GS, Grant DM, Mokaya R. Hydrogen storage in high surface area carbons: experimental demonstration of the effects of nitrogen doping. J Am Chem Soc 2009;131(45):16493–9.

[14] Wang L, Yang FH, Yang RT. Hydrogen storage properties of B- and N-Doped microporous carbon. Aiche J 2009;55(7):1823–33.

[15] Yushin G, Dash R, Jagiello J, Fischer JE, Gogotsi Y. Carbide-derived carbons: effect of pore size on hydrogen uptake and heat of adsorption. Adv Funct Mater 2006;16(17):2288–93.

[16] Mpourmpakis G, Froudakis GE, Lithoxoos GP, Samios J. SiC nanotubes: a novel material for hydrogen storage. Nano Lett 2006;6(8):1581–3.

[17] Barghi SH, Tsotsis TT, Sahimi M. Hydrogen sorption hysteresis and superior storage capacity of silicon-carbide nanotubes over their carbon counterparts. Int J Hydrogen Energy 2014;39(36):21107–15.

[18] Barghi SH, Tsotsis TT, Sahimi M. Experimental investigation of hydrogen adsorption in doped silicon-carbide nanotubes. Int J Hydrogen Energy 2016;41(1):369–74.

[19] Sun LY, Gong KC. Silicon-based materials from rice husks and their applications. Industrial Eng Chem Res 2001;40(25):5861–77.

[20] Lee JG, Cutler IB. Formation of silicon-carbide from rice hulls. Am Ceram Soc Bull 1975;54(2):195–8.

[21] Bhat BVR, Sanghi GP. Increase in the yield of silicon-carbide whiskers from rice husk. Bull Mater Sci 1987;9(4):295–303.

[22] Hanna SB, Mansour NAL, Taha AS, Abdallah HMA. Silicon-carbide and nitride from rice hulls .3. Formation of silicon-nitride. Trans J Br Ceram Soc 1985;84(1):18–21.

[23] Patel M, Kumari P. Silicon-carbide from sugarcane leaf and rice straw. J Mater Sci Lett 1990;9(4):375–6.

[24] Heo Y-J, Park S-J. Synthesis of activated carbon derived from rice husks for improving hydrogen storage capacity. J Industrial Eng Chem 2015;31:330–4.

[25] Ganesan A, Mukherjee R, Raj J, Shaijumon MM. Nanoporous rice husk derived carbon for gas storage and high performance electrochemical energy storage. J Porous Mater 2014;21(5):839–47.

[26] Ehrburger P, Addoun A, Addoun F, Donnet JB. Carbonization of coals in the presence of alkaline hydroxides and carbonates - formation of activated carbons. Fuel 1986;65(10):1447–9.

[27] Urabe Y, Ishikura T, Kaneko K. Development of porosity in carbons from yeast grains by activation with alkali metal carbonates. J Colloid Interface Sci 2008;319(1):381–3.

[28] Jagiello J, Olivier JP. 2D-NLDFT adsorption models for carbon slit-shaped pores with surface energetical heterogeneity and geometrical corrugation. Carbon 2013;55:70–80.

[29] Centeno TA, Stoeckli F. The assessment of surface areas in porous carbons by two model-independent techniques, the DR equation and DFT. Carbon 2010;48(9):2478–86.

[30] Patel M, Karera A. SiC whiskers from rice husk - role of catalysts. J Mater Sci Lett 1989;8(8):955–6.

[31] Zhiqiang L, Aixiang X, Tenglv Z. Energy from combustion of rice straw: status and challenges to China. Energy Power Eng 2011;3:325–31.

[32] Krstic VD. Production of fine, High-purity beta silicon-carbide powders. J Am Ceram Soc 1992;75(1):170–4.

[33] NarcisoRomero FJ, RodriguezReinoso F. Synthesis of SiC from rice husks catalysed by iron, cobalt or nickel. J Mater Sci 1996;31(3):779–84.

[34] Su J, Gao B, Chen Z, Fu J, An W, Peng X, et al. Large-scale synthesis and mechanism of β-SiC nanoparticles from rice husks by low-temperature magnesiothermic reduction. ACS Sustain Chem Eng 2016;4(12):6600–7.

[35] Janghorban K, Tazesh HR. Effect of catalyst and process parameters on the production of silicon carbide from rice hulls. Ceram Int 1999;25(1):7–12.

[36] Krishnarao RV. Effect of cobalt catalyst on the formation of SiC from rice husk silica-carbon black mixture. J Mater Sci 1995;30(14):3645–51.

[37] Martinez V, Valencia MF, Cruz J, Mejia JM, Chejne F. Production of beta-SiC by pyrolysis of rice husk in gas furnaces. Ceram Int 2006;32(8):891–7.

[38] Sevilla M, Mokaya R. Energy storage applications of activated carbons: supercapacitors and hydrogen storage. Energy Environ Sci 2014;7(4):1250–80.

[39] Bhat VV, Contescu CI, Gallego NC. Kinetic effect of Pd additions on the hydrogen uptake of chemically-activated ultramicroporous carbon. Carbon 2010;48(8):2361–4.

[40] Zhang H, Bhat VV, Feng PX, Contescu CI, Gallego NC. Effect of potassium-doping on the microstructure development in polyfurfuryl alcohol - derived activated carbon. Carbon 2012;50(14):5278–85.

[41] Cabria I, Lopez MJ, Alonso JA. Enhancement of hydrogen physisorption on graphene and carbon nanotubes by Li doping. J Chem Phys 2005;123(20):20471.

[42] Schindler BJ, LeVan MD. The theoretical maximum isosteric heat of adsorption in the Henry's law region for slit-shaped carbon nanopores. Carbon 2008;46(4):644–8.

[43] Wang X, Liew KM. Hydrogen storage in silicon carbide nanotubes by lithium doping. J Phys Chem C 2011;115(8):3491–6.

[44] Fujino T, Fuse T, Ryu JT, Inudzuka K, Yamazaki Y, Katayama M, et al. Observation of hydrogen adsorption on 6H-SiC(0001) surface. Appl Surf Sci 2001;169:113–6.

[45] Takami J, Naitoh M, Yokoh I, Nishigaki S, Toyama N. STM and LEED observation of hydrogen adsorption on the 6H-SiC(0001)3 x 3 surface. Surf Sci 2001;482:359–64.

[46] Craig BI, Smith PV. The chemisorption of hydrogen on silicon and silicon-carbide (1 0 0) surfaces. Phys B 1991;170(1–4):518–22.

[47] Enoki T, Miyajima S, Sano M, Inokuchi H. Hydrogen alkali-metal graphite ternary intercalation compounds. J Mater Res 1990;5(2):435–66.

[48] Srinivas G, Zhu Y, Piner R, Skipper N, Ellerby M, Ruoff R. Synthesis of graphene-like nanosheets and their hydrogen adsorption capacity. Carbon 2010;48(3):630–5.

[49] Zheng Q, Wang X, Gao S. Adsorption equilibrium of hydrogen on graphene sheets and activated carbon. Cryogenics 2014;61:143–8.

[50] Foo KY, Hameed BH. Utilization of rice husks as a feedstock for preparation of activated carbon by microwave induced KOH and K_2CO_3 activation. Bioresour Technol 2011;102(20):9814–7.

[51] Deng H, Li GX, Yang HB, Tang JP, Tang JY. Preparation of activated carbons from cotton stalk by microwave assisted KOH and K_2CO_3 activation. Chem Eng J 2010;163(3):373–81.

[52] Foo KY, Hameed BH. Porous structure and adsorptive properties of pineapple peel based activated carbons prepared via microwave assisted KOH and K2CO3 activation. Microporous Mesoporous Mater 2012;148(1):191–5.